

Tetrazole-Functionalized Organoboranes Exhibiting Dynamic Intramolecular N→B-Coordination and Cyanide-Selective Anion Binding

Jonas Schepper,^[c] Andreas Orthaber,^[b] and Frank Pammer^{*,[a]}

Starting from two different cyano-functionalized organoboranes, we demonstrate that 1,3-dipolar [3 + 2] azide-nitrile cycloaddition can serve to generate libraries of alkyl-tetrazole-functionalized compounds capable of intramolecular N→B-Lewis adduct formation. Due to the relatively low basicity of tetrazoles, structures can be generated that exhibit weak and labile N→B-coordination. The reaction furnishes 1- and 2-alkylated regio-isomers that exhibit different effective Lewis-

acidities at the boron centers, and vary in their optical absorption and fluorescence properties. Indeed, we identified derivatives capable of selectively binding cyanide over fluoride, as confirmed by ¹¹B NMR. This finding demonstrates the potentialities of this synthetic strategy to systematically fine-tune the properties of lead structures that are of interest as chemical sensors.

Introduction

The exploitation of intramolecular dynamic processes is of increasing interest in current chemical research.^[1,2] For instance hemilabile coordination of chelating ligands to transition metals has been recognized as crucial for many catalytic processes,^[3–6] and was exploited in the development of sensing applications.^[7]

One of the greatest strengths of organic materials lies in their large structural variety and that gives rise to a broad range of physical and electronic properties. Recently, the introduction of main group elements is being investigated intensively in materials science and organic electronics to access new structural scaffolds and to exploit unusual electronic effects.^[8] Introduction of boron^[9–16] has attracted particular interest in this regard as it can be incorporated in either the tri-^[10,17–19] and

tetracoordinate^[20–29] form, which gives rise to different electronic and chemical properties.

Tricoordinate boron centers in pendant groups^[19,30–33] or embedded within π -systems^[34–37] lead to a lowering of the Lowest Unoccupied Molecular Orbital (LUMO) and hence increased electron affinity, due to conjugation with their p^z -orbital. Compounds featuring intramolecular N,C^2 -chelated tetracoordinate boron,^[29,38–45] also exhibit increased electron affinity, and have therefore been considered as electron-transporting (n-type) materials.^[20–29] Recently, they have attracted growing interest, due to promising results in organic light emitting devices,^[46] n-channel organic field effect transistors,^[47] and organic photovoltaic cells,^[20–27] and have been used to generate compounds with helical topology.^[48–50]

A key limitation in the exploration of organoboranes is the limited choice of methods for their preparation. Most commonly used are step-wise metalation,^[29,33,35,51–56] and electrophilic C–H-borylation.^[57,58] Hydroboration of suitable substrates can also yield a broad range of N→B-heterocycles.^[59–66]

Recently we developed strategies for the synthesis of N→B-heterocycles by building-up the N-heterocyclic component through cycloaddition-reactions. We found that both 1,3-dipolar [3 + 2] azide-alkyne cycloaddition^[67,68] and cobalt-mediated [2 + 2 + 2] cycloaddition between nitriles and alkynes^[69] are highly efficient tools for the preparation of electronically and structurally diverse N→B-ladder boranes.

In this paper we report the synthesis of N→B-ladder boranes through generation of tetrazoles through 1,3-dipolar [3 + 2] azide-nitrile cycloaddition. An intriguing feature of triazole-containing ladders generated through azide-alkyne cycloaddition is that the N→B-coordination is weak, and the system therefore exists in dynamic equilibrium with its conformer (Scheme 1). Labile coordination in N→B rings has also been observed in sterically congested systems,^[70] or strained systems,^[71,72] when the Lewis acidity at the boron center is reduced,^[73] or when weaker Lewis bases such as ethers^[74] or

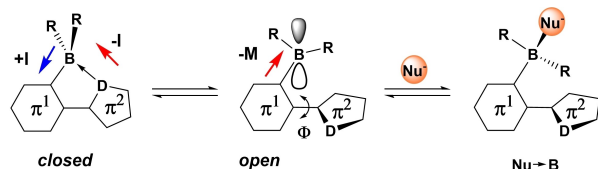
[a] PD Dr. F. Pammer
Helmholtz Institute Ulm
Karlsruhe Institute for Technology
Helmholtzstrasse 11, 89081 Ulm, Germany
E-mail: frank.pammer@kit.edu
Homepage: <https://hiu-batteries.de>

[b] Prof. Dr. A. Orthaber
Department of Chemistry – Ångström laboratories
Uppsala University
BOX 523, 75120 Uppsala, Sweden

[c] Dr. J. Schepper
Institute of Organic Chemistry II and Advanced Materials
Ulm University
Albert-Einstein-Allee 11, 89081 Ulm, Germany

Supporting information for this article is available on the WWW under <https://doi.org/10.1002/chem.202401466>

© 2024 The Authors. Chemistry - A European Journal published by Wiley-VCH GmbH. This is an open access article under the terms of the Creative Commons Attribution Non-Commercial NoDerivs License, which permits use and distribution in any medium, provided the original work is properly cited, the use is non-commercial and no modifications or adaptations are made.



Scheme 1. Electronic effects in **closed** ladder boranes and **open** tricoordinate boranes. D: Lewis basic donor atom.

carbonyl moieties^[75] are introduced, and if the formation of seven-membered N→B^[76] and O→B-rings^[77,78] is required.

Labile D→B- coordination (D: N, O, P, donor atom) can have a strong influence on the electronic properties of a given π -system (Scheme 1). In the **closed**, D→B-conformation, the π -system is planarized ($\Phi \approx 0^\circ$), and conjugation along the backbone is more effective. Also, the electron-rich tetracoordinate boron center acts as an inductive electron donor towards its carbon substituents (+I) and towards the π^1 -ring, while at the same time exerting an electron withdrawing effect (−I) onto the donor atom (D) in the π^2 -ring. In the **open** conformation, the empty p_z -orbital on boron exerts a strong electron withdrawing mesomeric effect (−M) on the π -system, while conjugation along the backbone is less efficient due to increased torsion ($|\Phi| \gg 0^\circ$). Furthermore, in the **open** conformation the boron center can act as Lewis acid that can bind nucleophiles (Nu→B). This latter property of organoboranes has been exploited to develop chemical sensors for various anions.^[79,80] In this report, we demonstrate that 1,3-dipolar [3+2] azide-nitrile cycloaddition can serve to generate compounds capable of labile intramolecular N→B-coordination and with vastly differing electronic and optical properties.

Results and Discussion

Synthesis and Structure

In this work we report the modification of two Mes₂B-functionalized aryl nitriles (Mes = Mesityl, 2,4,6-trimethylphenyl) – the previously reported *ortho*-borylated benzonitrile **B1**^[69] and the 1,8-functionalized naphthonitrile **N1** (Chart 1), which is newly introduced herein. **N1** was prepared in 2 steps starting from 1-naphthonitrile with an overall yield of 22% (see electronic supporting information, ESI, for details).

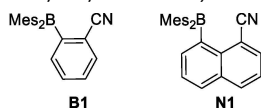


Chart 1. The boranes used as starting materials in this survey.

N1 shows a chemical shift of in ¹¹B NMR of 71 ppm, in the typical range for tri-aryl boranes (**B1**: 76 ppm^[69]). The Lewis-acidities of **N1** and **B1** were assessed by determining their acceptor numbers (AN) according to Gutmann and Becket^[81–83] – i.e. via the ³¹P NMR response of Et₃P=O to the presence of the respective borane – according to the empirical formula.

$$AN = 2.21 \times (\delta(^{31}\text{P}_{\text{Et}_3\text{PO} \rightarrow \text{B}}) - 41)$$

This experiment gave AN-values of 15.3 for **B1** and 14.7 for **N1** (for ³¹P NMR data see Figures S1 and S2 in the ESI). Both compounds therefore exhibit approximately equal Lewis acidity and are significantly less Lewis acidic than e.g. Ph₃B (AN ≈ 65),^[84] but are rather comparable to boric acid esters B(OR₃) (12 to 24).^[81]

Single crystals of **N1** suitable for crystallographic analysis by X-ray diffraction were obtained by slow evaporation of a THF solution. The resulting crystal structure shows the presence of a trigonal planar boron center. The both the BMes₂- and the CN-moiety are bent out of the naphthyl-plane (torsion B–C₈–C₁–CN: 25.4°) due to the steric pressure of the mesityl substituents (see Figure 1). This brings boron and the nitrile carbon atom 0.573 Å above and 0.234 Å below the naphthyl-plane, respectively. The crystal structure of **B1** has already been reported elsewhere.^[69]

B1 and **N1** served as starting materials for the preparation of a series of alkylated tetrazoles via a two-step-one-pot procedure (Scheme 2). The cyano-groups of both boranes can be converted into tetrazoles via a silver-mediated dipolar [3+2]-cycloaddition.^[85] The initially formed sodium salts (**B2**, **N2**) were alkylated *in situ* to yield the final products.^[86] Aqueous workup of **B2** also allowed isolation of the unsubstituted tetrazole **B3** in 86% yield. Subsequent alkylation of **B3** is also possible. However, the one-pot procedure provided much higher yields.

Alkylation of **B2** with sterically unhindered propyl- and benzyl-bromide generally yields a mixture of the 1- and 2-alkyl-tetrazoles in an approximate 1:1 ratio and a combined yield of 65–70% (**B4a/b**; **B5a/b**). Alkylation with 1-bromomethylpyrene furnished only the 2-alkyl-product **B6b** in a much lower yield of 23%. Conversion of the sterically more hindered **N1** with propyl- and benzyl-bromide almost exclusively yielded the 2-isomers in 20–30%. Still, the isolation of **N4a** in 2% yield shows that this regio-isomer can also form. All compounds were characterized by NMR and high-resolution mass-spectrometry. The regio-structure of all isomers was confirmed through the distinctive chemical shift of the tetrazole carbon in ¹³C NMR (see Figure S7 in the ESI) and ¹H NOE-NMR (see Figures S3 through S6 in the ESI), as well as through solid state structures of **B5a**, **B5b** and **N4b** obtained via single-crystal X-ray diffraction (see Figure 2 and Section 2.2.4 in the ESI).

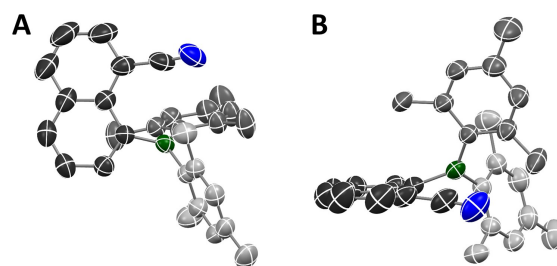
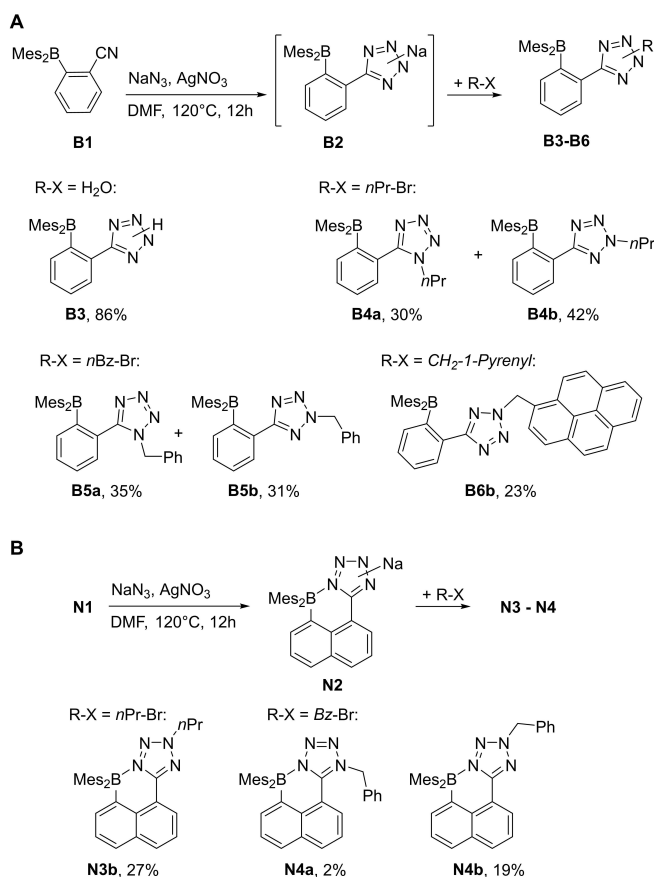
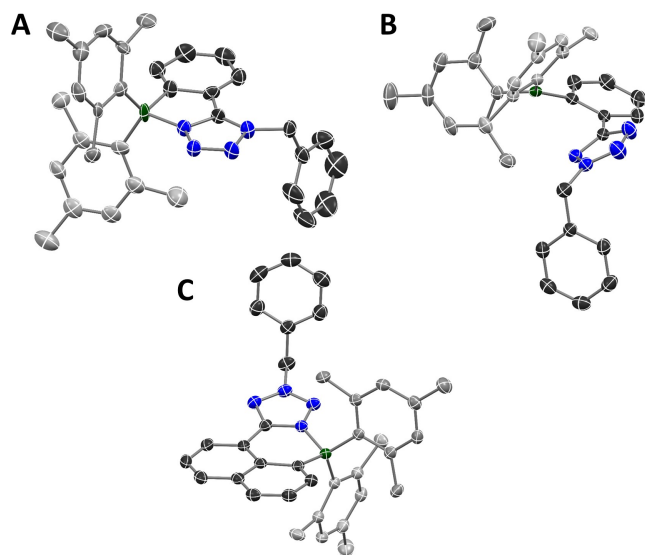


Figure 1. Crystal structure of compound **N1**. Top-down (A) and side-view (B). Ellipsoids shown at 50% probability level. Hydrogen atoms are omitted for clarity.



Scheme 2. Syntheses of tetrazole-functionalized boranes.

Figure 2. Crystal structures of compounds **B5a** (A) and **B5b** (B) and **N4b** (C); Ellipsoids shown at 50% probability level. Hydrogen atoms are omitted for clarity.

^{11}B NMR indicates chemical differences in the $\text{N}\rightarrow\text{B}$ -coordination (Table 1, see also Figure S8 and S9 in the ESI). The 1-substituted **B**-boranes show chemical shifts below 5 ppm (**B4a**: 1 ppm; **B5a**: 3.6 ppm both in THF), in the typical range of

tetracoordinate boron (-5 to $+10$ ppm).^[80] Contrarily, 2-substituted **B**-boranes exhibit signals between 15 and 20 ppm (**B4b**: 17 ppm; **B5b**: 21 ppm; **B6b**: 18.7 ppm, all recorded in THF). These latter values lie outside the typical ranges of tetracoordinate boron^[80] but are still much lower than expected for triaryl boranes (60 – 90 ppm),^{[87][88]} which indicates weak or labile $\text{N}\rightarrow\text{B}$ coordination. This observation would agree with the lower base strength of 2- over 1-alkyl tetrazoles.^[89]

In the **N**-boranes, tighter $\text{N}\rightarrow\text{B}$ -coordination is observed, as indicated by the upfield shifted ^{11}B NMR signals ($\delta\approx-2$ ppm). This conjecture is further corroborated by DFT calculations (Table 2, Scheme 3): A comparison of simulated structures of *open* (non-coordinated) and *closed* ($\text{N}\rightarrow\text{B}$ -coordinated) conformers consistently shows that closed geometries are highly favorable ($\Delta G_{\text{o/c}}\approx+32$ to $+38$ kJ/mol) for **N**-boranes, while 1-alkylated **B**-systems are close to thermo-neutral, and 2-alkylated **B**-boranes favor *open* structures. For 1-alkylated **B**-boranes the energetic differences between *open* and *closed* is low - ranging from $+7.3$ kJ/mol for **N4a** to -7.2 kJ/mol for **B5a**. Both conformers can therefore exist in dynamic equilibrium at ambient temperature. The 2-alkylated **B**-boranes (i.e. the “b” derivatives) can coordinate either via nitrogen atom **N1** or atom **N4**. However, coordination via **N1** is highly disfavored over **N4**-coordination by $+25$ – 40 kJ/mol (see Table 2, “ $\Delta G_{\text{o/c}}$ via **N1**” vs. “ $\Delta G_{\text{o/c}}$ via **N4**”).

The computed energetic differences between different conformers of **B5a** and **B5b** helps to explain why **B5a** adopts a *closed* geometry in the solid state, while **B5b** assumes an *open* one. The slightly unfavorable $\text{N}\rightarrow\text{B}$ -coordination of **B5a** ($\Delta G_{\text{o/c}}=-7.2$ kJ/mol) can be compensated by packing effects, while for **B5b** ($\Delta G_{\text{o/c}}=-15.7$ kJ/mol) this is not the case anymore.

In order to determine the strength of the rotational barriers variable temperature NMR (VT-NMR) experiment have been performed with compounds **B4a**, **B4b**, **B5a**, and **B5b** (see Figures S14–S16). At lower temperature, the ^1H NMR reveals the splitting of the signal of the aromatic mesityl protons into two, and later four signals. We assign this splitting-up to the slowing of the rotation around the $\text{C}_{\text{Mesityl}}\text{--B}$ bond. The coalescence temperatures (T_{c}) of 232 K (**B4a**), 234 K (**B4b**), 240 K (**B5a**), and 248 K (**B5b**) have been determined which correspond to rotational barriers of between 45.4 and 48.5 kJ/mol.

These values only correspond to the rotation of the mesityl-groups. However, rotation around the $\text{C}_{\text{Mes}}\text{--B}$ -bond is expected to be much less hindered in the open conformation, because of reduced steric crowding around **B** and a generally lower rigidity of the molecular. To assess the barrier of the actual aryl-

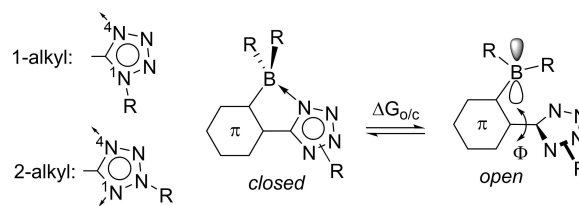
Scheme 3. Numbering, coordinating atoms, and *open* and *closed* conformers.

Table 1. Electrochemical and optical properties of the synthesized boranes.

Compnd.	$E_{\text{p}}^{\text{red[a]}}$ [V]	LUMO ^{SQW[b]} [eV]	$\lambda_{\text{max}}^{[c]}$ [nm]	λ_{onset} [nm]	$E_{\text{g}}^{\text{opt[d]}}$ [eV]	λ_{em} [nm]	Stokes shift ^[e] [cm ⁻¹]	$\Phi^{[f]}$ [%]	¹¹ B-NMR ^[g] [ppm]
B4a	−2.58	−2.52	314	352	3.52	444	9325	93	1.0
B4b	−2.66	−2.44	337	353	3.51	n. d.	–	–	17.0
B5a	−2.47	−2.63	312	357	3.47	454	10025	97	3.6
B5b	−2.39	−2.71	336	354	3.50	n. d.	–	–	21.0
B6b	n. d.	n. d.	346	381	3.25	377, 396, 418, 446	2377	2	18.7
N3b	−2.56	−2.54	360	392	3.16	n. d.	–	–	−1.7
N4b	−2.43	−2.67	363	393	3.16	n. d.	–	–	−1.7
N4a	n. d.	n. d.	n. d.	n. d.	n. d.	n. d.	n. d.	n. d.	−2.4

[a] Peak-potential relative to FcH/FcH⁺, determined via Square-Wave-Voltammetrie in THF with 0.1 M [NnBu₄][PF₆], scan-speed 100 mV/s;^[b] LUMO-Energy relative to Ferrocene (−5.1 eV);^[c] Longest wave-length absorption maximum. Shoulder bands determined by Gaussian deconvolution; See ESI for details;^[d] Derived from the absorption onset;^[e] Derived from λ_{max} and λ_{em} ; ^[f] Measured with an integrating sphere;^[g] Recorded in THF-d₈.

Table 2. Overview over computational results.

Com- pnd.	$d_{\text{N} \rightarrow \text{B}}^{[a]}$ via N4 [Å]	$\Delta G_{\text{o/c}}^{[b]}$ via N4 [kJ/mol]	$d_{\text{N} \rightarrow \text{B}}^{[a]}$ via N1 [Å]	$\Delta G_{\text{o/c}}^{[b]}$ via N1 [kJ/mol]	$d_{\text{N} \rightarrow \text{B}}^{[d]}$ XRD [Å]	FIA ^[e] [kJ/mol]		Charges in <i>open</i> conformers ^[f]			
						vs. <i>open</i> kJ/mol]	vs. N4- <i>closed</i> kJ/mol]	Mulliken		APT	
								Tetra- zole-C	B	Tetra- zole-C	B
1 B4a	1.657	1.6				326.9	325.3	−0.167	−0.055	0.388	1.118
2 B4b	1.683	−8.9	1.691	−40.9		300.3	309.2	−0.201	−0.142	0.298	1.114
3 B5a	1.654	−7.2			1.643(8)	318.2	325.4	−0.210	−0.068	0.406	1.128
4 B5b	1.682	−15.7	1.684	−42.2		286.0	301.6	−0.281	−0.095	0.295	1.11
5 B6b	1.666	−10.7	1.696	−34.8							
6 N3b	1.639	31.6	1.651	−1.9		287.2	255.6	−0.190	0.031	0.334	1.142
7 N4a	1.627	7.3				298.8	291.5	−0.124	−0.059	0.442	1.146
8 N4b	1.645	37.5	1.651	−0.4	1.637(1)	276.4	238.9	−0.215	0.020	0.34	1.125
9 Mes₃B						287.7			−0.411		1.139
10 Mes₂BPh						301.8			0.103		1.165
11 MesBPh₂						309.4			0.295		1.172
12 BPh₃						331.8			0.545		1.212

[a] N→B-bond lengths in simulated structures. [b] ΔG of *open* vs. *closed* conformations; [c] Tetrazole-nitrogen coordinated to boron; [d] Experimental bond lengths from crystal structures. [e] Fluoride ion affinities. Values for entries 1–8 calculated against the most stable conformer. See text for details. [f] Summed into heavy atoms.

tetrazole rotation, the rotation around this bond has been simulated by DFT calculations of methyl-capped models of **B4** (**B4a'** and **B4b'**). The 360 °C scan gave two barriers of 25–30 kJ/mol for the 2-akylated borane **B4b'**, which is low enough to allow full rotation of the tetrazole ring. For the 1-akylated compound **B4a'** two barriers of 30 kJ/mol and almost 75 kJ/mol were found at 336 and 162 °, respectively. The higher barrier corresponds to the 1-methyl group being forced past the Mes₂B-group and effectively blocks full rotations. The system could still oscillate over a roughly 300 ° range via the lower barrier.

Optical and Electrochemical Properties

The optical gaps of the B-tetrazoles ($E_{\text{g}}^{\text{opt}} \approx 3.5$ eV, Table 1) are generally larger than that of the parent borane **B1** (3.22 eV). The only exception is **B6b**, of which the optical properties are dominated by features originating from the pyrenyl-moiety (see Figure 3A). The N-boranes exhibit lower optical gaps, due to the more extended π -system.

Aside from the already reported borane **B1** only **B4a** and **B5a** and **B6b** were found to be fluorescent (see Figure 3B). The 1-alkylated B-boranes exhibit very similar spectra and with quantum yields of 93 and 97% respectively. Fluorescence in **B6b** is weak ($\Phi=2\%$) and attributed to emission from the

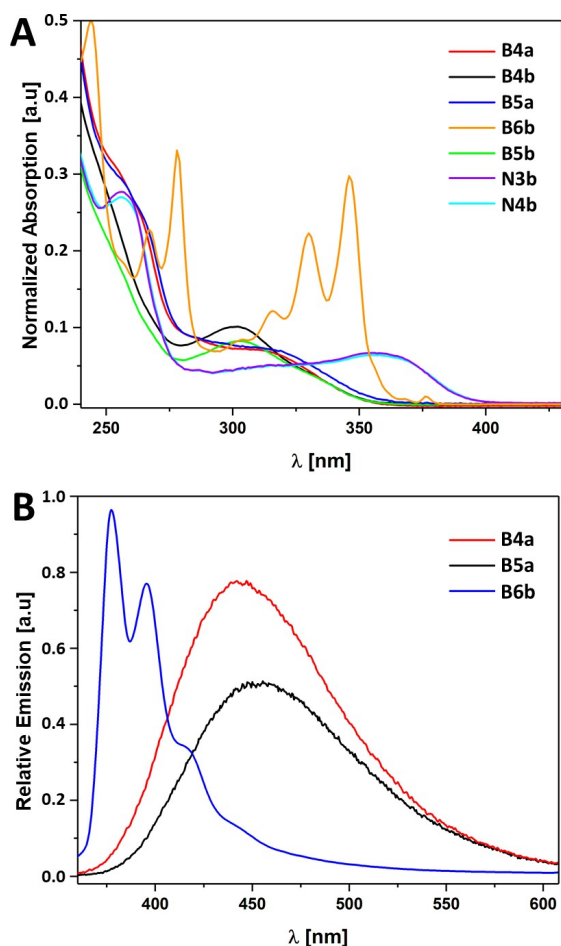


Figure 3. UV-vis absorption (A) and fluorescence (B) spectra recorded in dichloromethane.

pyrene-moiety, which is not conjugated to the π -system conjugated to boron.

Electrochemical analyses of the boranes by cyclic voltammetry (CV) and square-wave voltammetry (SWV) revealed that their reduction potentials are generally more negative and less reversible than those of the parent borane (e.g. **B1**: reversible, $E_p = -2.22$ V^[69] vs. FcH/FcH⁺^[90] **B4a**: irreversible, $E_p = -2.58$ V, **B4b**: quasi-reversible, $E_p = -2.66$ V, E_p = peak potentials determined by SWV). These values lie in the range of non-acceptor-substituted triarylboranes.^[67,68] Evidently, the alkyl-tetrazole-substituents are less able to stabilize a negative charge, than the cyano-group in parent system, even though the π -system is expanded through conjugation onto the tetrazole. Tailoring of the properties of the borane through this strategy may therefore only serve to lower its Lewis acidity and electron affinity, unless additional electron withdrawing substituent can be introduced on the tetrazole ring.

Anion Binding

In order to investigate the different N \rightarrow B interaction strengths in the different boranes, [nBu₄N]F and [nBu₄N]CN were added in

excess to the different tetrazoles, and the corresponding ¹¹B NMR spectra were recorded (see Figure 4, see also Figures S10–S13 in the ESI). The NMR experiments show no reaction of the boranes **B4a**, **B4b**, **B5a**, **B5b** to the presence of fluoride, while the presence of CN[−] resulted in the emergence of sharp signals at −10 to −20 ppm for the same four phenyl-tetrazoles. This signal shift indicates binding of cyanide to the boron centers.^[80] **B6b** shows the formation of a fluoride adduct upon addition of [nBu₄N]F (see Figure S12). The sterically more crowded naphthyltetrazoles **N3b** and **N4b** bind neither cyanide nor fluoride.

CN[−] and F[−] typically exhibit comparable binding to boron-based Lewis acids, and examples for selective binding of CN[−] are quite rare.^[91,92]

Following up on the NMR-studies on fluoride and cyanide binding, the optical response of the boranes **B4a**, **B4b**, **B5a** and **B5b** (see Figures S18A–D in the ESI) to the presence of CN[−] was also investigated. In the absorption spectra, binding of CN[−] to boron manifests in the suppression of the respective longest wavelength absorption bands (312 to 337 nm) and increase of a band centered around 280 nm. This would be consistent with the loss of conjugation to the empty p_z-orbital on boron, which generally lowers the LUMO. However, the steric pressure of CN-binding might also effect a larger torsion between the Mes₂B-substituted phenylene-ring and the tetrazole, which would also result in a blue-shift due to less effective conjugation.

Titration of the fluorescent boranes **B4a** and **B5a** showed a successive suppression of the emission that corresponds to CN[−]-binding (see Figure 5, see also section 2.2.4 of the ESI). Fitting with a 1 : 1 stoichiometry vs. CN[−] gave binding constants log(K) of 4.59 and 5.10, respectively, but showed poor agreement with the experimental data (see Figure S20). Fitting with a 1 : 2 stoichiometry vs. CN[−] gave quantitative agreement and log(K) values of 8.50 for **B4a** and 9.36 for **B5a** (see Figure S21).

To put these experimental binding constants into context, fluoride ion binding affinities (FIA)^{[93][94][94]} were calculated by DFT for **B4a/b**, **B5a/b**, **N3b** and **N4a/b** (Table 2). Mes₃B, Mes₂BPh, MesBPh₂ and BPh₃ (Table 2, entries 9–12) are included for reference. For the boranes the FIAs are given relative both *open* and *closed* conformers. The most relevant value is of course the one related to the most stable conformer, which in

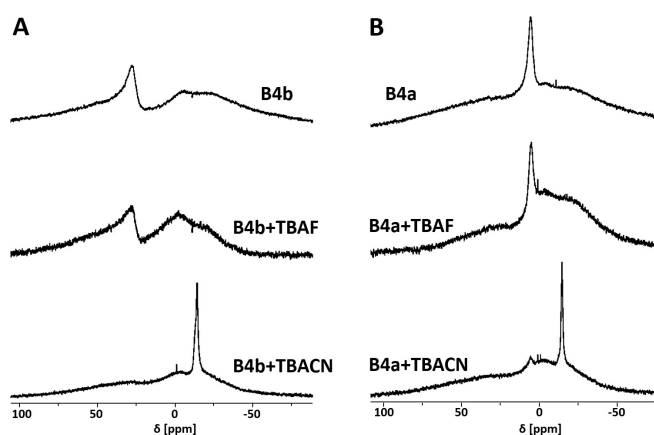


Figure 4. ¹¹B NMR spectra of neat boranes and after addition of F[−] and CN[−] salts.

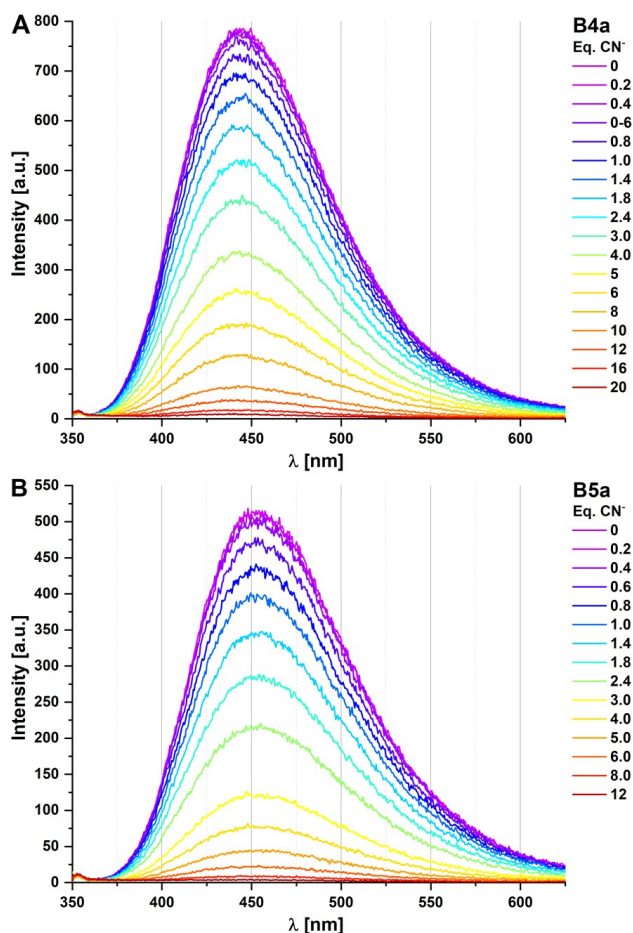


Figure 5. Fluorescence spectra showing the titration of phenyltetrazoles **B4a** (A), **B5a** (B) with NBu_4CN (TBACN); recorded in DCM.

turns is the lower absolute value given for each compound. Overall, the 1-alkylated “Ba” compounds’ (**B4a** = 325.3 kJ/mol, **B5a** = 318.2 kJ/mol) FIAs that were significantly higher than those of Mes_2BPh (301.8 kJ/mol) or MesBPh_2 (309.4 kJ/mol) but rather approach the binding strength of BPh_3 (331.4 kJ/mol). The 2-alkylated “Bb” boranes (**B4b** = 300.3 kJ/mol, **B5b** = 286.0 kJ/mol) gave values between those of Mes_2BPh and Mes_3B (287.7 kJ/mol). In line with the absence of anion binding in the experimental tests, FIAs of the naphthylboranes (**N3b** = 255.6 kJ/mol, **N4a** = 291.5 kJ/mol, **N4b** = 238.9 kJ/mol.) were found to be much lower.

These results show that the regio-chemistry on the tetrazole ring has a significant impact on the Lewis acidity. This may be owed to an inductive influence of the tetrazole ring. A comparison of atomic charges (Mulliken and ATP, Table 2) consistently showed higher (less negative) charges on boron and on the tetrazole-Cs of **B4a** and **B5a** than for **B4b** and **B5b**. Moreover, the calculations indicate that the Lewis acidity of the tetrazole-functionalized boranes can be varied over a range comparable to Mes_3B vs. BPh_3 , even with marginally functional substituents like alkyl and benzyl. This corroborates our hypothesis, that a readily functionalized N→B scaffold can serve to tailor the Lewis acidity of a given lead structure.

Conclusions

We have demonstrated a new and atom economic method to generate libraries of chemically and structurally diverse organo-boranes through 1,3-dipolar [3 + 2] azide-nitrile cycloaddition. The ensuing molecular geometries allow intramolecular N→B-coordination. However, we have shown that systems exhibiting strong and static, or weak and labile coordination can be obtained, depending on the structure of the starting material, and the regioisomer generated in the cycloaddition reaction. This allows to tailor the effective Lewis acidity of the organo-borane with comparative ease.

Of particular interest in this context, is our finding that we can prepare moderately Lewis-acidic boranes that discriminate between different types of anions and selectively bind cyanide (CN^-) over fluoride (F^-) as proven by ^{11}B NMR, and monitored by UV-vis absorption and fluorescence spectroscopy. The systems investigated in this survey showed only hypsochromic shifts in absorption spectra and suppression of photoluminescence. However, further synthetic exploration of this strategy may allow to identify compounds with a more distinctive and practical optical response, like turn-on fluorescence. We are currently exploring this avenue.

Supporting Information

The supporting information contains descriptions of materials and instruments used, detailed synthetic procedures, and additional analytical data not depicted in the main article. The latter includes NMR (^1H , ^{13}C , ^{11}B , NOE), optical spectra, electrochemical data, mass spectrometry data, optimized computed structures and detailed results of anion binding studies. The complete crystallographic data for **N1**, **B5a**, **B5b**, and **N4b** have been deposited with the Cambridge Crystallographic Data Centre under CCDC 2314044–2314047 and can be accessed via www.ccdc.cam.ac.uk/data_request/cif. Comprehensive supporting information has been uploaded to <https://zenodo.org> and can be accessed under DOI: 10.5281/zenodo.10974307.

Crystallographic data for has also been uploaded at the Cambridge Crystallographic Data Center (CCDC, <https://www.ccdc.cam.ac.uk/>) under deposition numbers CCDC-2314044 through CCDC-2314047 for compounds **B5b**, **N4b**, **B5a**, and **N1**, respectively.

The authors have cited additional references within the Supporting Information.^[95–102]

Acknowledgements

JS and FP thank the German Science Foundation (DFG, German Research Foundation, project number FP 2217/4-1) and the German Chemical Industry Fund (FCI, Liebig scholarship to FP) for financial support. Prof. Orthaber thanks the Swedish Research Council (Vetenskapsrådet) for support. Open Access funding enabled and organized by Projekt DEAL.

Conflict of Interests

The authors declare no conflict of interest.

Data Availability Statement

The data that support the findings of this study are openly available in Zenodo at 10.5281/zenodo, reference number 10974307.

Keywords: boranes · tetrazoles · 1,3-dipolar cycloaddition · anion sensors · Lewis acids

- [1] W. Zhang, Y. Jin, *Dynamic Covalent Chemistry: Principles, Reactions, and Applications*, John Wiley & Sons, Hoboken, 2017.
- [2] M. Barboiu, Ed., *Constitutional Dynamic Chemistry*, Springer Berlin Heidelberg, Berlin, Heidelberg, 2012.
- [3] A. J. M. Miller, *Dalton Trans.* 2017, 46, 11987–12000.
- [4] S. M. Mansell, *Dalton Trans.* 2017, 46, 15157–15174.
- [5] C. S. Slone, D. A. Weinberger, C. A. Mirkin, 1999, pp. 233–350.
- [6] A. Bader, E. Lindner, *Coord. Chem. Rev.* 1991, 108, 27–110.
- [7] S. E. Angell, C. W. Rogers, Y. Zhang, M. O. Wolf, W. E. Jones, *Coord. Chem. Rev.* 2006, 250, 1829–1841.
- [8] T. Baumgartner, F. Jäkle, *Main Group Strategies towards Functional Hybrid Materials*, John Wiley & Sons, 2008.
- [9] A. Doshi, F. Jäkle, in *Compr. Inorg. Chem. II*, Elsevier, 2013, pp. 861–891.
- [10] Y. Ren, F. Jäkle, *Dalton Trans.* 2016, 45, 13996–14007.
- [11] F. Jäkle, 2015, pp. 297–325.
- [12] F. Jäkle, *Coord. Chem. Rev.* 2006, 250, 1107–1121.
- [13] F. Jäkle, *Chem. Rev.* 2010, 110, 3985–4022.
- [14] F. Jäkle, in *Encycl. Inorg. Chem.* (Ed.: R. B. King), Wiley & Sons Ltd, 2005.
- [15] C. D. Entwistle, T. B. Marder, *Chem. Mater.* 2004, 16, 4574–4585.
- [16] C. D. Entwistle, T. B. Marder, *Angew. Chem.* 2002, 114, 3051.
- [17] E. A. Patrick, W. E. Piers, *Chem. Commun.* 2020, 56, 841–853.
- [18] E. von Grotthuss, A. John, T. Kaese, M. Wagner, *Asian J. Org. Chem.* 2018, 7, 37–53.
- [19] L. Ji, S. Griesbeck, T. B. Marder, *Chem. Sci.* 2017, 8, 846–863.
- [20] X. Long, J. Yao, F. Cheng, C. Dou, Y. Xia, *Mater. Chem. Front.* 2019, 3, 70–77.
- [21] X. Long, Z. Ding, C. Dou, J. Liu, L. Wang, *Mater. Chem. Front.* 2017, 1, 852–858.
- [22] R. Zhao, C. Dou, Z. Xie, J. Liu, L. Wang, *Angew. Chem. Int. Ed.* 2016, 55, 5313–5317.
- [23] X. Long, Y. Gao, H. Tian, C. Dou, D. Yan, Y. Geng, J. Liu, L. Wang, *Chem. Commun.* 2017, 53, 1649–1652.
- [24] X. Long, Z. Ding, C. Dou, J. Zhang, J. Liu, L. Wang, *Adv. Mater.* 2016, 28, 6504–6508.
- [25] J. Miao, Y. Wang, J. Liu, L. Wang, *Chem. Soc. Rev.* 2022, 51, 153–187.
- [26] C. Dou, J. Liu, L. Wang, *Sci. China Chem.* 2017, 60, 450–459.
- [27] M. Grandl, J. Schepper, S. Maity, A. Peukert, E. von Hauff, F. Pammer, *Macromolecules* 2019, 52, 1013–1024.
- [28] M. Vanga, A. Sahoo, R. A. Lalancette, F. Jäkle, *Angew. Chem.* 2022, 134, DOI 10.1002/ange.202113075.
- [29] A. Wakamiya, T. Taniguchi, S. Yamaguchi, *Angew. Chem.* 2006, 118, 3242–3245.
- [30] D.-T. Yang, J. Radtke, S. K. Møllerup, K. Yuan, X. Wang, M. Wagner, S. Wang, *Org. Lett.* 2015, 17, 2486–2489.
- [31] D. R. Levine, M. A. Siegler, J. D. Tovar, *J. Am. Chem. Soc.* 2014, 136, 7132–7139.
- [32] C. Reus, S. Weidlich, M. Bolte, H.-W. Lerner, M. Wagner, *J. Am. Chem. Soc.* 2013, 135, 12892–12907.
- [33] A. Wakamiya, K. Mori, S. Yamaguchi, *Angew. Chem. Int. Ed.* 2007, 46, 4273–4276.
- [34] T. Kushida, S. Yamaguchi, *Organometallics* 2013, 32, 6654–6657.
- [35] X. Yin, J. Chen, R. A. Lalancette, T. B. Marder, F. Jäkle, *Angew. Chem.* 2014, 126, 9919–9923.
- [36] X. Yin, F. Guo, R. A. Lalancette, F. Jäkle, *Macromolecules* 2016, 49, 537–546.
- [37] V. M. Hertz, N. Ando, M. Hirai, M. Bolte, H.-W. Lerner, S. Yamaguchi, M. Wagner, *Organometallics* 2017, 36, 2512–2519.
- [38] E. Poverenov, N. Zamoshchik, A. Patra, Y. Ridelman, M. Bendikov, *J. Am. Chem. Soc.* 2014, 136, 5138–5149.
- [39] P. Zalar, Z. B. Henson, G. C. Welch, G. C. Bazan, T. Nguyen, *Angew. Chem. Int. Ed.* 2012, 51, 7495–7498.
- [40] S. Hayashi, A. Asano, T. Koizumi, *Polym. Chem.* 2011, 2, 2764.
- [41] F. Focante, P. Mercandelli, A. Sironi, L. Resconi, *Coord. Chem. Rev.* 2006, 250, 170–188.
- [42] G. C. Welch, G. C. Bazan, *J. Am. Chem. Soc.* 2011, 133, 4632–4644.
- [43] W. Fraenk, T. M. Klapötke, B. Krumm, P. Mayer, H. Piotrowski, M. Vogt, *Zeitschrift für Anorg. und Allg. Chemie* 2002, 628, 745.
- [44] M. J. G. Lesley, A. Woodward, N. J. Taylor, T. B. Marder, I. Cazenobe, I. Ledoux, J. Zyss, A. Thornton, D. W. Bruce, A. K. Kakkar, *Chem. Mater.* 1998, 10, 1355–1365.
- [45] M. Fontani, F. Peters, W. Scherer, W. Wachter, M. Wagner, P. Zanella, *Eur. J. Inorg. Chem.* 1998, 1453–1465.
- [46] S. Wang, D. Yang, J. Lu, H. Shimogawa, S. Gong, X. Wang, S. K. Møllerup, A. Wakamiya, Y. Chang, C. Yang, Z. Lu, *Angew. Chem. Int. Ed.* 2015, 54, 15074–15078.
- [47] R. Hecht, J. Kade, D. Schmidt, A. Nowak-Król, *Chem. Eur. J.* 2017, 23, 11620–11628.
- [48] X. Zhang, F. Rauch, J. Niedens, R. B. da Silva, A. Friedrich, A. Nowak-Król, S. J. Garden, T. B. Marder, *J. Am. Chem. Soc.* 2022, 144, 22316–22324.
- [49] D. Volland, J. Niedens, P. T. Geppert, M. J. Wildervanck, F. Full, A. Nowak-Król, *Angew. Chem. Int. Ed.* 2023, 62, DOI 10.1002/anie.202304291.
- [50] F. Full, Q. Wölflick, K. Radacki, H. Braunschweig, A. Nowak-Król, *Chem. Eur. J.* 2022, 28, DOI 10.1002/chem.202202280.
- [51] S.-B. Ko, J.-S. Lu, S. Wang, *Org. Lett.* 2014, 16, 616–619.
- [52] D.-T. Yang, Y. Shi, T. Peng, S. Wang, *Organometallics* 2017, 36, 2654–2660.
- [53] M. Stanoppi, A. Lorbach, *Dalton Trans.* 2018, 47, 10394–10398.
- [54] Y.-L. L. Rao, H. Amarne, J.-S. S. Lu, S. Wang, *Dalton Trans.* 2013, 42, 638–644.
- [55] Y.-L. Rao, S. Wang, *Organometallics* 2011, 30, 4453–4458.
- [56] Y.-L. Rao, L. D. Chen, N. J. Mosey, S. Wang, *J. Am. Chem. Soc.* 2012, 134, 11026–11034.
- [57] N. Ishida, T. Moriya, T. Goya, M. Murakami, *J. Org. Chem.* 2010, 75, 8709–8712.
- [58] S. A. Iqbal, J. Pahl, K. Yuan, M. J. Ingleson, *Chem. Soc. Rev.* 2020, 49, 4564–4591.
- [59] M. Grandl, B. Rudolf, Y. Sun, D. F. Bechtel, A. J. Pierik, F. Pammer, *Organometallics* 2017, 36, 2527–2535.
- [60] M. Grandl, Y. Sun, F. Pammer, *Chem. Eur. J.* 2016, 22, 3976–3980.
- [61] M. Grandl, T. Kaese, A. Krautsieder, Y. Sun, F. Pammer, *Chem. Eur. J.* 2016, 22, 14373–14382.
- [62] M. Grandl, Y. Sun, F. Pammer, *Org. Chem. Front.* 2018, 5, 336–352.
- [63] M. Grandl, J. Schepper, S. Maity, A. Peukert, E. von Hauff, F. Pammer, *Macromolecules* 2019, 52, 1013–1024.
- [64] F. Pammer, J. Schepper, J. Glöckler, Y. Sun, A. Orthaber, *Dalton Trans.* 2019, 48, 10298–10312.
- [65] M. Grandl, F. Pammer, *Macromol. Chem. Phys.* 2015, 216, 2249–2262.
- [66] K. Yuan, N. Suzuki, S. K. Møllerup, X. Wang, S. Yamaguchi, S. Wang, *Org. Lett.* 2016, 18, 720–723.
- [67] R. Koch, Y. Sun, A. Orthaber, A. J. Pierik, F. Pammer, *Org. Chem. Front.* 2020, 7, 1437–1452.
- [68] S. Schraff, Y. Sun, F. Pammer, *J. Mater. Chem. C* 2017, 5, 1730–1741.
- [69] J. D. W. W. Schepper, A. Orthaber, F. Pammer, *J. Org. Chem.* 2021, 86, 14767–14776.
- [70] J. Chen, R. A. Lalancette, F. Jäkle, *Chem. Eur. J.* 2014, 20, 9120–9129.
- [71] S. Schwendemann, R. Fröhlich, G. Kehr, G. Erker, *Chem. Sci.* 2011, 2, 1842.
- [72] G.-Q. Chen, F. Türkyilmaz, C. G. Daniliuc, C. Bannwarth, S. Grimme, G. Kehr, *Org. Biomol. Chem.* 2015, 13, 10477–10486.
- [73] C. T. Hoang, I. Prokes, G. J. Clarkson, M. J. Rowland, J. H. R. Tucker, M. Shipman, T. R. Walsh, *Chem. Commun.* 2013, 49, 2509.
- [74] S. J. Cassidy, I. Brettell-Adams, L. E. McNamara, M. F. Smith, M. Bautista, H. Cao, M. Vasiliu, D. L. Gerlach, F. Qu, N. I. Hammer, D. A. Dixon, P. A. Rupar, *Organometallics* 2018, 37, 3732–3741.
- [75] Y. Shi, J. Wang, H. Li, G. Hu, X. Li, S. K. Møllerup, N. Wang, T. Peng, S. Wang, *Chem. Sci.* 2018, 9, 1902–1911.
- [76] C. Zeng, K. Yuan, N. Wang, T. Peng, G. Wu, S. Wang, *Chem. Sci.* 2019, 10, 1724–1734.

- [77] Y. Cao, J. K. Nagle, M. O. Wolf, B. O. Patrick, *J. Am. Chem. Soc.* **2015**, *137*, 4888–4891.
- [78] Y. Cao, N. E. Arsenault, D. Hean, M. O. Wolf, *J. Org. Chem.* **2019**, *84*, 5394–5403.
- [79] Z. M. Hudson, S. Wang, *Acc. Chem. Res.* **2009**, *42*, 1584–1596.
- [80] C. R. Wade, A. E. J. J. Broomsgrove, S. Aldridge, F. P. Gabbaï, *Chem. Rev.* **2010**, *110*, 3958–3984.
- [81] M. A. Beckett, G. C. Strickland, J. R. Holland, K. S. Varma, *Polymer* **1996**, *37*, 4629–4631.
- [82] U. Mayer, V. Gutmann, W. Gerger, *Monatsh. Chem.* **1975**, *106*, 1235–1257.
- [83] I. B. Sivaev, V. I. Bregadze, *Coord. Chem. Rev.* **2014**, *270–271*, 75–88.
- [84] A. Adamczyk-Woźniak, M. Jakubczyk, A. Sporyński, G. Żukowska, *Inorg. Chem. Commun.* **2011**, *14*, 1753–1755.
- [85] P. Mani, A. K. Singh, S. K. Awasthi, *Tetrahedron Lett.* **2014**, *55*, 1879–1882.
- [86] J. Roh, K. Vávrová, A. Hrabálek, *Eur. J. Org. Chem.* **2012**, 6101–6118.
- [87] C. D. Good, D. M. Ritter, *J. Am. Chem. Soc.* **1962**, *84*, 1162–1166.
- [88] N. M. D. Brown, F. Davidson, J. W. Wilson, *J. Organomet. Chem.* **1981**, *209*, 1–11.
- [89] V. A. Ostrovskii, G. I. Koldobskii, R. E. Trifonov, in *Compr. Heterocycl. Chem. III* (Eds.: A. R. Katritzky, C. A. Ramsden, E. F. V. Scriven, R. J. K. Taylor), Elsevier, Oxford, **2008**, pp. 257–423.
- [90] C. M. Cardona, W. Li, A. E. Kaifer, D. Stockdale, G. C. Bazan, *Adv. Mater.* **2011**, *23*, 2367–2371.
- [91] E. Ramachandran, S. A. A. Vandarkuzhali, G. Sivaraman, R. Dhamodharan, *Chem. A Eur. J.* **2018**, *24*, 11042–11050.
- [92] Y. Liu, J. Shi Du, S. Long Qi, L. Bao Zhu, Q. Biao Yang, H. Xu, Y. Xian Li, *Luminescence* **2021**, *36*, 336–344.
- [93] P. Erdmann, J. Leitner, J. Schwarz, L. Greb, *ChemPhysChem* **2020**, *21*, 987–994.
- [94] K. O. Christe, D. A. Dixon, D. McLemore, W. W. Wilson, J. A. Sheehy, J. A. Boatz, *J. Fluorine Chem.* **2000**, *101*, 151–153.
- [95] W. L. Armarego, D. D. Perrin, *Purification of Laboratory Chemicals*, Butterworth-Heinemann, Oxford, **1997**.
- [96] G. R. Fulmer, A. J. M. Miller, N. H. Sherden, H. E. Gottlieb, A. Nudelman, B. M. Stoltz, J. E. Bercaw, K. I. Goldberg, *Organometallics* **2010**, *29*, 2176–2179.
- [97] S. Ando, T. Matsuura, *Magn. Reson. Chem.* **1995**, *33*, 639–645.
- [98] P. Mani, A. K. Singh, S. K. Awasthi, *Tetrahedron Lett.* **2014**, *55*, 1879–1882.
- [99] I. V. Bliznets, A. A. Vasil'ev, S. V. Shorshnev, A. E. Stepanov, S. M. Lukyanov, *Tetrahedron Lett.* **2004**, *45*, 2571–2573.
- [100] B. Akhlaghinia, S. Rezazadeh, *J. Braz. Chem. Soc.* **2012**, *23*, 2197–2203.
- [101] B. Du, X. Jiang, P. Sun, *J. Org. Chem.* **2013**, *78*, 2786–2791.
- [102] G. M. Sheldrick, *Acta Crystallogr. Sect. A* **2008**, *64*, 112–122.

Manuscript received: April 15, 2024

Accepted manuscript online: May 6, 2024

Version of record online: June 14, 2024